Stochastic Receptor Expression Allows Sensitive Bacteria to Evade Phage Attack. Part II: Theoretical Analyses

E. Chapman-McQuiston and X. L. Wu
Department of Physics and Astronomy, University of Pittsburgh, Pittsburgh, Pennsylvania

ABSTRACT Stochastic gene expression in bacteria can create a diverse protein distribution. Most of the current studies have focused on fluctuations around the mean, which constitutes the majority of a bacterial population. However, when the bacterial population is subject to a severe selection pressure, it is the properties of the minority cells that determine the fate of the population. The central question is whether phenotype heterogeneity, such as a spread in the expression level of a critical protein, is sufficient to account for the persistence of the bacteria under the selection. A related question is how long such persistence can last before genetic mutation becomes significant. In this work, survival statistics of a bacterial population with a diverse phage-receptor number distribution is theoretically investigated when the cells are subject to phage pressures. The calculations are compared with our experimental observations presented in Part I in this issue. The fundamental basis of our analysis is the Berg-Purcell theoretical result for the reaction rate between a phage particle and a bacterium with a discrete number of receptors, and the observation that most phage-resistant mutants isolated in laboratory cultures are defective in phage binding. It is shown that a heterogeneous bacterial population is significantly more fit compared to a homogeneous population when confronting a phage attack.

INTRODUCTION

Heterogeneity in protein expression among genetically homogeneous prokaryotic and eukaryotic cells is an important biological phenomenon and has recently become a major area of biomedical interest (1–4). Protein-level population heterogeneity has been shown to allow a minority of the bacterial cells to survive even in instances when a saturating amount of antibiotics has killed most cells in the population (5). From these studies, simple mathematical models have been developed to provide insight on how these bacterial populations respond to sudden environmental stresses (5–7). These models have focused on systems where there are only two states of the cells, either sensitive or insensitive to the stress. In this article, we theoretically investigate population dynamics of *Escherichia coli* (*E. coli*) bacterium and λ-phage when sensitivity of the bacteria to phage infection has a broad, continuous distribution. As discussed in the accompanying article, referred to as Part I, this continuous spectrum of susceptibility arises because phage adsorption depends on the number of λ-receptors (LamB) on the bacterium, and this number can fluctuate in time in a single cell and in different bacteria due to stochastic gene expression and cell division (8,9). The biological underpinning of such fluctuations is perhaps the stochastic gene expression and unequal partitioning of proteins during cell division. For a given phage pressure, defined as the number of initial phages per volume $P(0)$, the bacteria with a high number of receptors are infected rapidly and are eliminated from the population whereas bacteria with a low number of receptors are less prone to infection and have the chance to multiply. The population dynamics is akin to a prey-predator model (10–12) but the process in this case is highly nonlinear; we note that even though only a single successful phage binding is required to infect a bacterium, the high-receptor-number cells are able to bind multiple phages and effectively alleviate the phage pressure for low-receptor-number cells. The latter population, therefore, is protected not only by virtue of its low binding rate but is also shielded by the high-receptor-number cells.

Based on our earlier phage adsorption studies (13), a mathematical model is constructed that incorporates essential features of phage infection, which includes the heterogeneity of LamB receptors in the bacterial population, the switching of bacteria from high (low) to low (high) receptor subpopulations, and multiplications of bacteria and phage. It is shown that the naïve homogeneous population model, which has been previously used for interpreting bacterium/phage population dynamics data (14), leads to bacterial extinction even for a moderate phage pressure. Including receptor heterogeneity can significantly improve the fitness of the bacterial population and allows it to persist under strong phage pressures. This robust bacterial response was found to be the case even when the phenotype switching is neglected in the population model. In this simple case, an analytical expression can be developed which shows that bacteria with high receptor numbers are decimated but those with low receptor numbers are able to grow for a wide range of phage pressures $P(0)$. The critical receptor number n_C that separates these two groups of cells is given by $n_C \approx \pi(a/s)((4\pi aDP(0)/\Lambda) - \ln(2a/b))^{-1}$, where a and b are the major and the minor semi-axis of the bacterium, s is the radius of the receptor,

Submitted September 12, 2007, and accepted for publication January 14, 2008.

Address reprint requests to X. L. Wu, Physics Dept. of Physics and Astronomy, University of Pittsburgh, 3941 Ohara Street, Pittsburgh, PA 15260. Tel.: 412-624-0873; E-mail: xlwu@pitt.edu.

Editor: Arup Chakraborty.

0006-3495/08/06/4537/12 $2.00
doi: 10.1529/biophysj.107.121723

D is the diffusion coefficient of the phage, and Λ is the growth rate of the bacterium. We found that the simplified model describes rather well the initial response of the bacterial population to various phage pressures, which we termed the ''killing curve'' in Part I (see this issue). Though our current measurements could not yield detailed information on phenotype switching, such as the switching rate and its dependence on the state of individual cells, several lines of evidence suggests that such phenotype switching does take place and is important for the bacterium/phage population dynamics. The switching appears to contribute to the appearance of a quasi-steady state of bacterial population in some intermediate timescales, where the bacterial growth rate is effectively zero for several generations, and to increase the threshold for bacterial extinction. Both of these effects cannot be accounted for by the heterogeneous model without phenotype switching. Our preliminary measurements further suggest that the switching process is rather slow, taking many generations for a bacterium to switch from a low receptor-number to a high receptor-number state under a severe phage pressure.

In the following, a phenomenological theory motivated by the known interactions between bacterium and phage is presented. The population dynamic equation for the bacterial population composed of varying degrees of phage sensitivity, which we termed the ''heterogeneous model'', is derived. It is shown that the equation can be reduced to the homogeneous one that was extensively used by earlier investigators (10–12,14). The heterogeneous model is sufficiently complex and its prediction is possible only via numerical integration. To understand the biological and physical basis of the model and its relation to the experiment, several approximations of varying degrees of rigor are explored and the results are compared with the measurements described in Part I in this issue.

MATHEMATICAL MODELING

Bacteria have developed a variety of natural defense mechanisms that target diverse steps of the phage life cycle, notably: blocking adsorption; preventing DNA injection; restricting incoming DNA; and having abortive infection systems. In this article, we investigate quantitatively the long-suspected scenario that the short-time persistence to phage infection occurs at the binding stage, the bacterium's first line of defense. We wish to show via systematic measurements and mathematical modeling that our observed behavior (the ''killing curves'') can be accounted for by this single mechanism. Previous theoretical (15) and experimental works (13,16) have shown that the phage adsorption rate of a bacterium is a function of the number of receptors n on the bacterial cell wall,

$$\gamma_n = \gamma_\infty \frac{ns}{ns + \frac{\pi a}{\ln(2a/b)}}, \quad (1)$$

where $\gamma_\infty = 4\pi Da/\ln(2a/b)$ is the adsorption rate for an ideal elliptical absorber whose entire surface is covered with receptors, D is the diffusion coefficient of the phage, and $s(\approx 4$ nm) is the radius of the receptor. This remarkable result was first derived by Berg and Purcell (15) and was later found to be valid essentially for a wide range of receptor coverage (17). The adsorption exhibits two different behaviors: For low receptor numbers, $n \ll n_0(\equiv \pi(a/s)/\ln(2a/b))$, the rate constant is linear in n, $\gamma_n \approx \gamma_1 n$, suggesting no interference between different receptors on phage binding, where $\gamma_1 = 4Ds$ is the adsorption rate of a single receptor on the bacterium. For high receptor numbers $n \gg n_0$, $\gamma_n \approx \gamma_\infty$, which is independent of n. The existence of a linear crossover is by itself interesting as it suggests that even sparsely populated receptors are sufficient to achieve a high reaction rate. This surprising result can be shown to be a general property of diffusion, i.e., once a phage touches a surface, it has a high probability of probing the surface many times before leaving (13,15). Using parameters for the bacterial strain Ymel used in the experiment, $\bar{a} = 2.1$ μm, $\bar{b} = 0.46$ μm, and $D = 7.6 \times 10^{-8}$ cm^2/s (see Section A in Supplementary Material, Data S1 in Part I), we found n_0 to be $\sim$750, which is greater than the mean receptor number $\bar{n} \sim 270$. Very little is known about stochasticity of *lam*B expression in *E. coli*. However, judging from our flow cytometry data from Part I, it is evident that LamB fluctuates widely in different cells and under different growth conditions. Such wide cell-to-cell variations can create a broad spectrum of susceptibility to phage infection in a population. Our aim below is to show that bacterial survival statistics can, in part, be accounted for by the receptor number fluctuations.

Model equations

Heuristically, the population dynamics of bacterium and phage is akin to prey and predator communities and may be mimicked as such by the Lotka-Volterra equation (18). However, because the interactions between the bacterium and phage are reasonably well known, a more detailed/realistic model can be constructed. Let us assume for the moment that bacterial population is homogeneous and that at a given time the bacteria can be divided into the sensitive population S and the infected (pre- and post-bursting) population I in the presence of a phage population P. The equations describing these three populations are determined by the second-order rate equations and are given by

$$\frac{dS(t)}{dt} = (\Lambda - \gamma P(t))S(t), \quad (2)$$

$$\frac{dI(t)}{dt} = \gamma P(t)S(t) - \varepsilon I(t), \quad (3)$$

$$\frac{dP(t)}{dt} = m\gamma P(t-\tau)S(t-\tau) - \gamma P(t)(S(t) + I(t)), \quad (4)$$

where Λ is the bacterial growth rate, γ is the phage adsorption rate, τ is the phage maturing time, $\varepsilon(\leq 1/\tau)$ is the infected-cell

degradation rate, and m is the bursting size. In the above, we have assumed that the sensitive cells have a growth rate Λ that is independent of the phage pressure $P(t)$ and that the adsorption is irreversible with γ given by Eq. 1 with n being the average number of receptors. In a previous theoretical study of *E. coli* and λ-phage population dynamics (14), a four-population model was proposed, where the infected cell population I was subdivided into pre- and post-bursting populations. It can be shown, however, that the four-population model is equivalent to our three-population model. For simplicity, in the following the three-population model will be used. Aside from ε, all the parameters in Eqs. 2–4 are known, and in principle it should allow detailed comparisons between theory and experiment. Indeed, such an attempt has been made in Rabinovitch (14), where the investigators found that under reasonable conditions, a limit cycle can exist and thus coexistence between bacterium and phage is feasible. However, our calculations indicate that coexistence between bacterium and phage requires a fine-tuning of the rate constants in Eqs. 2–4 and are thus not robust solutions of the population dynamics. Given the experimental conditions in our measurements, we found that the homogeneous model consistently yields extinction of the bacterial population even for a moderate $P(0)$. To reconcile with the experimental observation, which show persistence of sensitive cells under large phage pressures, population heterogeneity of bacteria to phage infection are introduced. Specifically we consider number fluctuations of the LamB receptors, i.e., the bacteria with n receptors, having the same sensitivity to phage infection, are grouped together and designated as the subpopulation B_n, where $0 < n < N_{max}$. Within each subpopulation, the bacteria are further classified into sensitive cells S_n and infected cells I_n, similar to the homogeneous model. The number conservation law then dictates the following set of equations must hold,

$$\frac{dS_n}{dt} = (\Lambda - \gamma_n P)S_n + \sum_{m=0}^{N_{max}}{}'\alpha_{nm}S_m - \left(\sum_{m=0}^{N_{max}}{}'\alpha_{mn}\right)S_n, \quad (5)$$

$$\frac{dI_n}{dt} = \gamma_{n+1}(S_{n+1} + I_{n+1})P - \gamma_n I_n P - \varepsilon I_n, \quad (6)$$

$$\frac{dP}{dt} = mP(t-\tau)\sum_{n=0}^{N_{max}}\gamma_n S_n(t-\tau) - P\sum_{n=0}^{N_{max}}\gamma_n(S_n + I_n), \quad (7)$$

where γ_n is the adsorption coefficient given by Eq. 1, α_{mn} is the switching rate from subpopulation n to subpopulation m, and the prime in the sum indicates that $m = n$ is excluded. The switching between the subpopulations arises due to insertion or decay of receptors on the cell wall and due to partitioning of receptors during cell division. A schematic drawing depicting different bacterial subpopulations is given in Fig. 1. It is useful to point out certain limitations of our model. First of all, it is assumed that the growth rate Λ for different bacterial subpopulations is the same. This assumption is consistent with the observation that in the presence of a moderate amount of maltose or glucose, which is the case in the current experiment, the receptor number n is not the limiting factor for cell growth (19). In the special case of maltose-limiting media, the n-dependent growth rate can be taken into account by changing Λ to Λ_n, where Λ_n is also expected to depend on n as in Eq. 1. Second, the equations assume the carrying capacity of the medium is infinite, which is reasonable for the current experiment because our killing curves were measured in ~10 h, and the overall bacterial concentration is well below saturation ($\sim 10^9$ cm^{-3}) during measurements. Equations 5–7 are complicated since they consist of $2(N_{max}+1)$ equations with many rate constants, such as α_{mn}, being unknown. However, since our measurement is only sensitive to total uninfected bacteria $S(t) = \sum_{n=0}^{N_{max}} S_n(t)$ by counting colonies on agar plates, Eq. 1 can be significantly simplified. Summing on both sides of Eq. 5 and recognizing that the switching terms cancel,

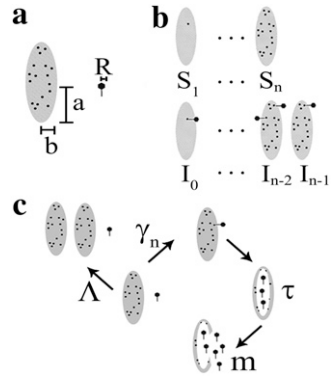

FIGURE 1 (*a*) The drawing depicts the parameters of the bacteria and phage used to determine the adsorption coefficient. (*b*) The subpopulation of sensitive bacteria with n receptors is labeled as S_n, and the subpopulation of infected bacteria that have n available free receptors is labeled as I_n. (*c*) The life cycles of bacterium and phage. Uninfected or sensitive bacteria will multiply at a rate Λ. They adsorb phage at a rate γ_n, which depends on the receptor number n. Infected bacterium cannot multiply but can adsorb more phage with the rate determined by their available free receptors. After a latent period τ, the infected bacteria will burst, releasing m phage into the environment.

$$\sum_{n=0}^{N_{max}}\sum_{i=0}^{N_{max}}{}'\alpha_{ni}S_i - \sum_{n=0}^{N_{max}}\left(\sum_{i=0}^{N_{max}}{}'\alpha_{in}\right)S_n = 0. \quad (8)$$

Equation 5 now reads $dS/dt = \Lambda S - P\sum_{n=0}^{N_{max}}\gamma_n S_n$. We next define an ensemble-averaged adsorption rate $\bar{\gamma}_S(t) \equiv \sum_{n=0}^{N_{max}}\gamma_n S_n/S$, which is time-dependent. The population dynamic equation for the sensitive bacteria is finally given by

$$\frac{dS}{dt} = [\Lambda - \bar{\gamma}_S(t)P(t)]S(t). \quad (9)$$

The equations for the infected cells and the free phage population can be similarly derived with the result

$$\frac{dI}{dt} = \bar{\gamma}_S(t)P(t)S(t) - \varepsilon I(t), \quad (10)$$

$$\frac{dP}{dt} = mP(t-\tau)\bar{\gamma}_S(t-\tau)S(t-\tau) - P(t)[\bar{\gamma}_S(t)S(t) + \bar{\gamma}_I(t)I(t)], \quad (11)$$

where $\bar{\gamma}_I = \sum_{n=0}^{N_{max}} \gamma_n I_n / I$ is the average adsorption coefficient of the infected cell population. We have thus shown that it is feasible to reduce the $2(N_{max}+1)$ equations to merely three equations, and most significantly, the new equations have no explicit switching dependence. The cost of such simplification, however, is the appearance of the time-dependent adsorption constant $\gamma(t)$. We noticed that Eqs. 9–11 are identical to the homogeneous model, Eqs. 2–4, if the time-dependent adsorption rates are set to a constant $\bar{\gamma}_S(t) = \bar{\gamma}_I(t) = \gamma$. This illustrates the similarity as well as the fundamental differences between the two models, and calls into question the very assumption that interaction parameters and rate constants are time-independent in early models of population dynamics. Although the switching terms do not appear explicitly in Eq. 9, as we will show below, bacterial switching from one subpopulation to another is an important dynamic attribute and is relevant for a quantitative understanding of bacterium/phage populations as a function of time. However, we will also show that even in its absence ($\alpha_{mn} = 0$), the heterogeneous model already yields robust responses for the bacteria population to different phage pressures, and it can mimic the killing curves more closely than the homogeneous model.

Approximate solutions to the model equations

Without the switching terms, Eqs. 5–7 can be integrated numerically for the given initial bacterial distribution $S_n(0) = B_n(0)$, which we determined by the flow cytometry measurements. Here the only unknown is the receptor degradation rate ε, which is treated as an adjustable parameter. A fourth-order Runge-Kutta algorithm from Numerical Recipes in C was implemented in the numerical integration (20). The detailed comparison between the numerical method and our experimental results is presented in the next section.

Although numerical integration of Eqs. 5–7 is straightforward when $\alpha_{mn} = 0$, it is difficult to gain insights about the biological/physical processes governing the dynamics of the heterogeneous population. Considerable progress can be made, however, if one assumes that the phage population remains constant $P(t) = P(0) = P_o$. Such an assumption allows the sensitive bacterial populations $S_n(t)$ in Eq. 5 to be decoupled from the rest of the populations, i.e., Eqs. 6 and 7, making analytical analyses possible. The assumption of constant phage pressure, though not generally satisfied in our measurements, is valid under certain limiting conditions, such as for very short-time population dynamics ($t \ll \min[1/\bar{\gamma}(0)P_o 1/\bar{\gamma}(0)S(0)]$) when phage are not significantly depleted by adsorption, and for very high phage concentrations ($P_o \gg \sum_n nS_n(0)$) as if a phage reservoir were present. Under these conditions, the term $\Lambda - \gamma_n P_o$ is constant and each sensitive bacterial subpopulation obeys the simple equation

$$S_n(t) = S_n(0)\exp[(\Lambda - \gamma_n P_o)t]. \quad (12)$$

We noted that without phenotype switching, $S_n(t)$ is either growing or decaying exponentially depending on whether the effective growth rate $\Lambda_{eff} = \Lambda - \gamma_n P_o$ is positive or negative. For a given P_o, one can define the critical receptor number n_C such that for those subpopulations with $n > n_C$, $S_n(t)$ decays with time whereas for those subpopulations with $n < n_C$, $S_n(t)$ increases with time. Here n_C is given by

$$n_C = \frac{\pi a/s}{\left(\frac{\gamma_\infty P_o}{\Lambda} - 1\right)\ln(2a/b)}, \quad (13)$$

which is plotted in Fig. 2. One observes that n_C increases sharply as P_o is decreased. Since the maximum number of receptors is approximately a thousand, this calculation shows that for $P_o < 5 \times 10^6$ cm^{-3}, essentially all bacterial subpopulations grow exponentially. Such peculiar behavior can be understood by the fact that for $n \gg n_0[\equiv \pi(a/s)/\ln(2a/b)] \sim 750$, the adsorption rate γ_n becomes independent of n and a minimal phage concentration $\sim 5 \times 10^6$ cm^{-3} is required to have a noticeable effect on bacterial growth. It is also interesting to calculate the phage pressure that is required to inhibit growth of the $n = 1$ subpopulation. Using

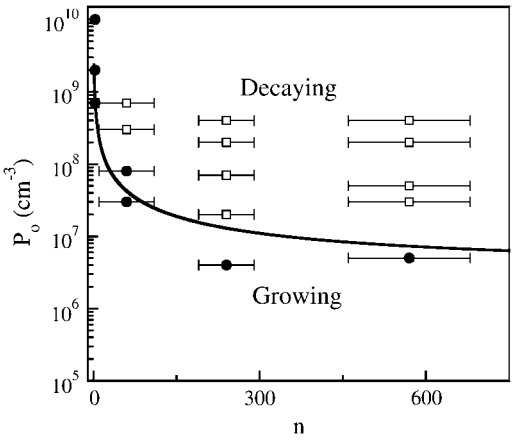

FIGURE 2 The life-and-death of bacterial subpopulations with n receptors subjected to different phage pressures P_o. The figure depicts the threshold value for a bacterial subpopulation with n receptors to grow or to decay. For P_o above the line, the population decays but for P_o below the line, the population grows. The threshold values are calculated based on the experimental parameters for Ymel, which are listed in Table 1 of Part I. This threshold curve matches rather well with the experimentally measured short-time (when $\bar{\gamma}$approximately constant) growth and decay rates for Ymel and LE392 populations when P_o and n are varied systematically. As discussed in the main text, the initial behavior of a heterogeneous population is equivalent to a homogeneous one characterized by the mean receptor number $\bar{n}$. In the figure, the circles (*squares*) correspond to population growth (decay) for various combinations of P_o and $\bar{n}$. Different $\bar{n}$ in the experiment were obtained by growing LE392 bacteria in different media.

Eq. 13, we found that when $n_C = 1$, $P_o \approx 3 \times 10^9$ cm^{-3}, which is surprisingly close to the mutant selection limit $P_o \sim 10^{10}$ cm^{-3} found in our Part I.

An interesting feature of Eq. 13 is that it is independent of the bacterial concentration, implying that this criterion is necessary but may not be sufficient for inhibiting bacterial growth for the entire population. To inhibit bacterial growth, including those with only one receptor, it also requires that for each receptor, at least one free phage is available for binding. This additional condition $P_o \gg \sum_n nS_n(0)$ turns out to be identical to the presence of a phage reservoir (or the constant P condition) discussed above. This relation can be cast into a simpler form: $P_o \gg \bar{n}S(0)$ or MOI($\equiv P(0)/S(0)$) $\gg \bar{n}$. For instance, for $P_o \approx 3 \times 10^9$ cm^{-3} and $\bar{n} \approx 300$, $S(0)$ must $\ll 10^7$ cm^{-3} for the constant-P assumption to be valid. As we will see below, this condition is satisfied in some but not all of our measurements. When the above constant-P condition is supplemented with the kinetic requirement $P(t)\ \gamma_1 > \Lambda$, one obtains the sufficient condition for decimating the entire sensitive population: $P(t) > \max(\bar{n}S(t), \Lambda/\gamma_1)$. For practical reasons, such as in mutant selection or perhaps in future phage therapy, this relation provides a useful guide for experiment or treatment designs.

We next calculate the time-dependent bacterial population in the presence of a constant phage pressure and examine the effect of receptor distribution on the fitness of the bacterial population as a whole. This can be done by summing over all subpopulations $S_n(t)$ given by Eq. 12,

$$S(t) = \sum_{n=0}^{N_{max}} S_n(0)\exp[(\Lambda - \gamma_n P_0)t]. \tag{14}$$

To illustrate the effect of receptor number fluctuations on the fitness, we used the Gaussian function for the receptor distribution

$$p(n) \equiv \frac{S_n(0)}{S(0)} = \sqrt{\frac{2}{\pi\sigma^2}}\exp\left[-\frac{(n-\bar{n})^2}{2\sigma^2}\right]\frac{H(n)}{erfc(-\bar{n}/\sqrt{2}\sigma)}, \tag{15}$$

where $H(n)$ is the Heaviside step function and $p(n)$ is properly normalized for $n \geq 0$. The Gaussian distribution is rare in biological systems but has been observed in systems when proteins are expressed at very high levels (21,22). A full treatment using a log-normal distribution, which is closer to our experimental observations, is given in Section A in Data S1. Changing the summation in Eq. 14 to an integral and assuming $\gamma_n = \gamma_1 n$, which is a good approximation when $\bar{n}$ is $\ll n_0$, $S(t)$ can be calculated by a straightforward integration,

$$S(t) = S(0)\exp[(\Lambda - \gamma_1\bar{n}P_o)t + \frac{1}{2}(\gamma_1\sigma P_o)^2 t^2]\frac{erfc\left(\frac{\gamma_1 P_o\sigma t}{\sqrt{2}} - \frac{\bar{n}}{\sqrt{2}\sigma}\right)}{erfc\left(-\frac{\bar{n}}{\sqrt{2}\sigma}\right)}, \tag{16}$$

where $erfc(x)$ is the complementary error function, which is a monotonically decreasing function of x and has the following limits: $erfc(x\rightarrow-\infty) = 2$ and $erfc(x\rightarrow\infty) = 0$. The behavior of $S(t)$ is thus determined predominantly by the exponential function for short and intermediate times. However, for long times, $erfc(x)$ becomes important and $S(t\rightarrow\infty) \propto \exp(\Lambda t)/t$. One finds that in the absence of receptor-number fluctuations, $\sigma = 0$, $S(t)$ is the solution for a homogeneous population, which has an effective growth exponent $\Lambda_{eff} = \Lambda - \gamma_1\bar{n}P_o$ that can be either positive or negative depending on the phage pressure P_o and $\bar{n}$. The receptor-number fluctuations ($\sigma \neq 0$) always favor the recovery of the bacterial population, but its effect only takes place at an intermediate time because of its quadratic t dependence. For a declining bacterial population, $\Lambda_{eff} = 0$, the recovery occurs when $t > \tau\left[\equiv 2(\gamma_1\bar{n}P_o - \Lambda)/(\gamma_1\sigma P_o)^2\right]$. In the presence of a strong phage pressure, $\gamma_1\bar{n}P_o \gg \Lambda$, $\tau = (2/\gamma_1\sigma P_o)(\bar{n}/\sigma)$, showing recovery occurs earlier for a broader receptor distribution. Useful information can also be extracted in the short-time limit $t \ll \tau$, where one can find the average number of receptors $\bar{n}$ by plotting Λ_{eff} versus P_o. The slope of such a plot yields $\gamma_{\bar{n}}$ (or $\bar{n}$) and the intercept is the unperturbed growth rate Λ. The above calculation, though very simplified, illustrates the importance of receptor-number fluctuations on the survival or the fitness of the bacterial population.

Comparisons between theory and experiment

In the following, theoretical expressions developed above are compared with measurements. This allows us to evaluate the validity as well as the weaknesses of certain assumptions made in the model. More importantly, it allows us to gain insight about the phenotype switching, which while difficult to model, is biologically significant.

Killing curves with P *approximately constant*

We first examine the killing-curve under the assumption of constant P and no phenotype switching $\alpha_{mn} = 0$. In this case, $S(t)$ in Eq. 14 only depends on the initial receptor distribution $p(n) = S_n(0)/S(0)$. To satisfy the condition $P(t) \approx P_o$, we compared calculations with measurements carried out at a large phage concentration $P_o \sim 1.5 \times 10^8$ cm^{-3} and a relatively small bacterial concentration $S(0) \sim 10^6$ cm^{-3}. A typical measurement for Ymel is displayed in Fig. 3, where the circles are for $S(t)$ and the squares are for $P(t)$. We note that though MOI$>\bar{n}$ is not strictly obeyed, the MOI is sufficiently large to render $P(t)$ approximately constant over the span of 7 h. During this time interval, $S(t)$ plummeted by nearly two orders of magnitude. The solid line in the figure is the fit to the theoretical expression given in Data S1, where $p(n)$ is assumed to be log-normally distributed. The fitting procedure yields the mean $m = \overline{\ln(n)} = 5.4 \pm 0.1$ and the standard deviation $\sigma' = \overline{[\ln(n) - \langle\ln(n)\rangle]^2}^{1/2} = 0.78 \pm 0.02$ for the log-normal distribution. Based on this distribution, the

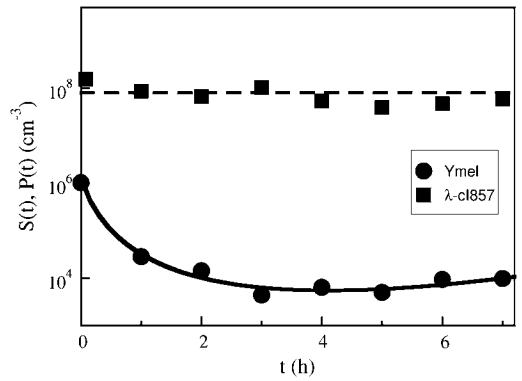

FIGURE 3 A killing curve with a constant phage pressure. The circles are for Ymel population $S(t)$ measured in CFU/cm^3 and the squares are for the phage concentration $P(t)$ measured in PFU/cm^3. The solid line is the fit to the log-normal receptor distribution using Eq. S5 in Data S1. More than three curves such as this one were fit and the resulting $\bar{n}$ and σ are listed in Table 1.

normal mean $\bar{n}$ and the standard deviation $\sigma(\equiv\sqrt{(\overline{n^2}-\bar{n}^2)})$ can be calculated. Averaging over seven separate runs, we found $\bar{n} = 310 \pm 20$ and $\sigma = 320 \pm 30$. Five similar measurements were also performed for LE392, resulting in $\bar{n} = 600 \pm 120$ and $\sigma = 610 \pm 130$. We found that while $\bar{n}$ obtained above is reasonably consistent with the flow cytometry measurements (see Table 1 for more details), σ is nearly a factor-of-two greater for both strains of bacteria. The discrepancy is in part due to the fact that the lower end of the $p(n)$ determined by flow cytometry cannot be accurately mimicked by the simple log-normal function (see Fig. 2 *c* in Part I), and in part due to the presence of switching in the bacterial subpopulations; a subject we will come back to below. Both of these factors conspire to give an artificially large σ and make the assumptions used to derive the analytic model only valid at short times, a subject investigated later in this article. However, considering the simplicity of the analytic model, the agreement between the calculation and the measurements is fair.

*Killing curves without the constant-*P *assumption*

In the more general case, the phage concentration P is not constant due to phage adsorption and production. Thus, it is of interest to examine the situation where the constant-*P* assumption is relaxed, but the switching terms are still suppressed $\alpha_{mn} = 0$. The population dynamics characterized by Eqs. 5–7 were numerically integrated using the flow cytometry data in Part I as the initial condition for each subpopulation S_n and the results are presented in Fig. 4, *b*, *e*, and *h*, for Ymel, induced LE392, and uninduced LE392, respectively. Other relevant parameters for the calculations were summarized in Table 1 of Part I, except for ε. Biologically, ε^{-1} is the LamB degradation time, which should be long compared to the bacterial lysis time, i.e., $\varepsilon^{-1} \geq \tau$. In the numerical integration, ε was varied over a broad range, and the features of the killing curve were found to be insensitive to large changes in ε. Hence, ε was fixed at τ^{-1}. For comparison, the dynamic equations for a homogeneous population, Eqs. 2–4, were also numerically integrated using the average receptor numbers, $\bar{n} = 250, 550,$ and 2, for Ymel, induced LE392, and uninduced LE392, respectively. The results for the homogeneous model are presented respectively in Fig. 4, *c*, *f*, and *i*, for the two strains of bacteria. In all calculations, $S(0)$ and $P(0)$ were given according to the experimental conditions in Fig. 4, *a*, *d*, and *g*. Namely, the colors of the individual curves in the calculations match that of the measurements.

The experimental results and model calculations for the uninduced LE392 bacteria are presented in Fig. 4, *g–i*. They are an example of persistence in the extreme form when a large percentage of the population is persistent against phage infection. There exists a critical phage pressure defined as $\Lambda_{eff}(\equiv\Lambda - \gamma_1\bar{n}P_C(0)) = 0$. For $\bar{n} = 2$ and when the increased growth rate $\Lambda = 1.3$ h^{-1} for cells grown in M9+glucose was taken into account, we found $P_C(0) = 2 \times 10^9$ cm^{-3}. This critical point has a large effect on the simulation of the homogeneous model as seen in Fig. 4 *i*, where three distinctive behaviors (growth, slow decay, and fast decay) are observed depending on whether $P(0)$ is greater than or less than $P_C(0)$. However, this strong $P(0)$ dependence was not observed in the experiment as displayed in Fig. 4 *g* nor predicted by the heterogeneous model as displayed in Fig. 4 *h*. For the heterogeneous model, when $P(0) > P_C(0)$, only a slight decrease in the growth rate in early times was observed, which is delineated by the black line in Fig. 4 *h*. The system very quickly recovers and resumes the expo-

TABLE 1 Mean and standard deviation of the receptor distribution

	Log-normal fits		Short-time fits		Flow cytometry		Fluorometry
	$\bar{n}$	σ_n	$\bar{n}$	σ_n	$\bar{n}$	σ_n	$\bar{n}$
LE392	600 ± 120	610 ± 130	618 ± 140	215 ± 25	570 ± 50	200 ± 10	550 ± 80
Ymel	310 ± 20	320 ± 30	177 ± 23	105 ± 8	240 ± 30	140 ± 60	270 ± 30

The average receptor number $\bar{n}$ and its standard deviation σ_n were obtained using four different methods: fitting to the early- and the intermediate-time killing data using the saddle-point approximation (the log-normal fits); fitting to the early killing data; using data from flow cytometry; and from fluorometry. The $\bar{n}$ for both LE392 and Ymel strains was also estimated using microscope measurements (data not shown) and was found to be consistent with the results obtained from fluorometry and in flow cytometry. While $\bar{n}$ is in generally good agreement between different measurements, σ_n has large variations. In particular, the log-normal fit yields anomalously big σ_n, which we discussed in the main text.

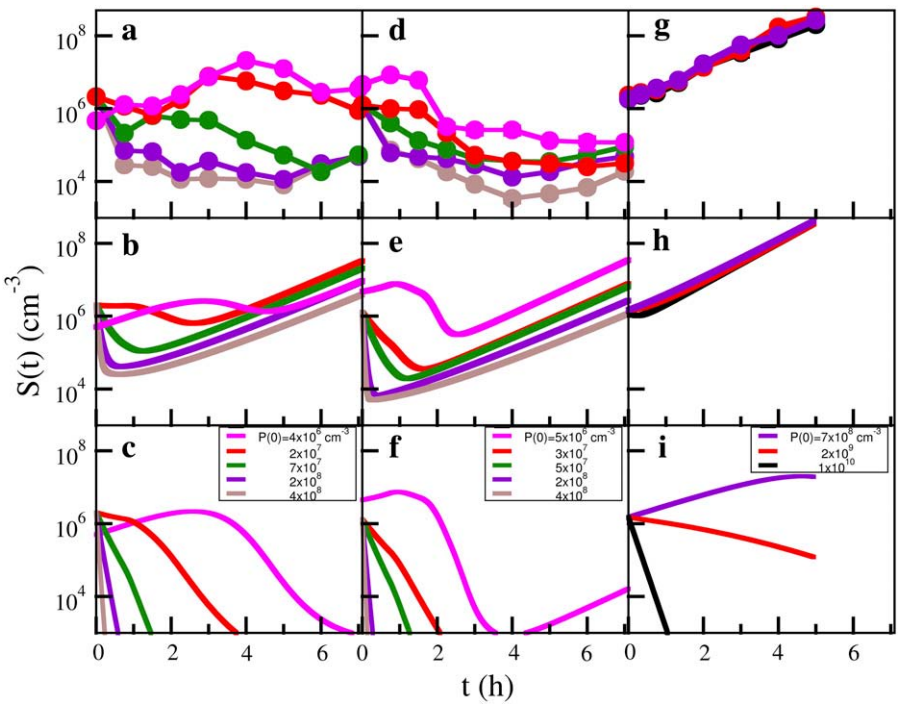

FIGURE 4 Comparison between simulations and experimental killing curves without the constant-P assumption. The initial bacterial concentration is $B(0) \approx 10^6$ cm^{-3} and is approximately the same for all runs. The curves in panel *a* are for Ymel with $P(0) = 4 \times 10^6$ (*pink*), 2×10^7 (*red*), 7×10^7 (*green*), 2×10^8 (*purple*), and 4×10^8 cm^{-3} (*brown*). The simulations using the heterogeneous model (Eqs. 5–7) and the homogeneous model (Eqs. 2–4) are displayed respectively in panels *b* and *c* for the corresponding $P(0)$ used in the experiment. The curves in panel *d* are for induced LE392 with $P(0) = 5 \times 10^6$ (*pink*), 3×10^7 (*red*), 5×10^7 (*green*), 2×10^8 (*purple*), and 4×10^8 cm^{-3} (*brown*). The simulations using the heterogeneous model and the homogeneous model are displayed respectively in panels *e* and *f* for the corresponding $P(0)$ used in the experiment. The curves in panel *g* are for uninduced LE392 with $P(0) = 7 \times 10^8$ cm^{-3} (*purple*), $P(0) = 2 \times 10^9$ cm^{-3} (*red*), and $P(0) = 10^{10}$ cm^{-3}. The simulations using the heterogeneous model and the homogeneous model are displayed, respectively, in panels *h* and *i* for the corresponding $P(0)$ used in the measurement. The relevant parameters used in the simulations are given in Table 1 of Part I. For uninduced LE392 bacteria, which were grown in M9+glucose, we used $\Lambda = 1.3\ \mathrm{h}^{-1}$ and $m = 30$, which were determined by experiment.

nential growth. Overall, the heterogeneous model mimics very well the experimental observation for all $P(0)$ used in the measurement.

Let us focus on the more subtle case of bacteria expressing a higher level of LamB, such as Ymel in Fig. 4 *b* and induced LE392 bacteria in Fig. 4 *e*. Different behaviors emerge in short times for these cells depending on $P(0)$. For a low $P(0)$, the bacterial population $S(t)$ initially grows with a positive growth rate Λ_{eff} that decreases with $P(0)$. For a high $P(0)$, $S(t)$ decreases and Λ_{eff} is negative. As shown in these figures, it is feasible to adjust $P(0)$ such that Λ_{eff} is nearly zero, indicating a rough balance between the killing and the reproduction of bacteria in short times. Over a longer timescale, $S(t)$ evolves in a more complicated fashion for low $P(0)$ than for high $P(0)$; it increases in size for a period of time, follows a period of decline, and then increases again. The late-time growth rate is approximately equal to Λ, indicating that those prospering bacteria have small number of n and their growth is largely unaffected by the presence of phage. The ups-and-downs in $S(t)$ over time are due to the multiplication of phage particles that alters the phage pressure $P(t)$ in the sample. In other words, these features will be absent if $P(t)$ is held constant. Such a phage perturbation is less noticeable when $P(0)$ is large initially. In this case, $S(t)$ always decreases in early times and then increases in the later time. The crossover from the early- to the late-time behavior becomes shorter as $P(0)$ increases as is expected based on the saddle-point analysis discussed above (see also Data S1). The above highly nonlinear features predicted by the heterogeneous population model mimics qualitatively the experimental observations displayed in Fig. 4, *a* and *d*. Quantitatively, however, the simulation and the measurements show noticeable differences, particularly the slow recovery in $S(t)$ when $P(0)$ is large. We wish to address this important feature later in the article.

We now turn our attention to the theoretical predictions for homogeneous bacterial populations, which are presented in Fig. 4, *c* and *f*, for Ymel and induced LE392, respectively. Here, one observes that as far as the short-time behavior is concerned, the homogeneous model makes reasonable predictions about when the bacterial population is growing (or decaying) when $P(0)$ is varied. The predicted magnitude of Λ_{eff} is also consistent with the above more detailed calculations. For instance, for Ymel with $\bar{n} = 250$, the critical phage concentration is predicted to be $P_{\mathrm{C}}(0) \sim 2 \times 10^7$ cm^{-3}, and for induced LE392 with $\bar{n} = 550$, $P_{\mathrm{C}}(0) = 8 \times 10^6$ cm^{-3}. These simple, quantitative features were indeed supported by extensive measurements as delineated in Fig. 2. Here the data points represent bacterial populations that are initially growing (*circles*) or decaying (*squares*), and the boundary between the two sets of data are well represented by the theoretical prediction, Eq. 13, which is plotted as the line. This observation leaves shows the population heterogeneity and fluctuations in $P(t)$ are insignificant in predicting the short-time population dynamics. This can be understood by the fact that the short-time response of $S(t)$ is mostly due to

the majority cell population, which is equivalent to a homogeneous population characterized by the mean receptor number $\bar{n}$ that remains approximately constant during the measurements. Since in short time there is no significant phage production or adsorption, $P(t)$ also remains nearly constant. A conspicuous but disturbing feature of the homogenous model is the late-time behavior, where even with a moderate $P(0)$, the sensitive bacteria suffer a rapid decline in the population size. It is clear that the homogeneous population lacks the plasticity to cope with the phage pressure, and it becomes extinct quickly under most of our experimental conditions. For a low phage pressure, however, recovery, oscillations, or even a steady-state solution were found to be feasible, but this requires fine tuning of the model parameters and thus cannot represent the true dynamics of our bacterium/phage system.

The above model calculations leave little doubt that population heterogeneity is a significant attribute for a bacterial population to evade phage attack for long times, i.e., over many generations of bacterial replications. The fact that most of these surviving bacteria, when regrown in a phage-free environment, recover their ability to adsorb phage, rules out the possibility of genetic mutation to be the cause of phage resistance seen in our experiment. For the initial bacterial population size S(0) $\sim 10^6$ cm^{-3}, which is used in most of our measurements as displayed in Fig. 4, mutants must be generated at timescales much longer than our measurement time $\sim$12 h. Our experiment thus supports the scenario that such coexistence is maintained by a group of bacteria that express receptors at a very low level such that their growth rate is not significantly affected by the presence of phage.

The effect of phenotype switching

The above discussion gives the impression that switching between bacterial subpopulations may not be significant since, even in its absence ($\alpha_{mn} = 0$), the simplified model (Eqs. 5–7) already captures essential features of the killing curves. In this section, however, we would like to show based on several lines of evidence that phenotype switching between subpopulations must exist, and that it plays a subtle but important role for bacterium/phage population dynamics.

A conspicuous feature of the killing curves in Fig. 4, *a* and *d*, is the broad minima seen in $S(t)$ when a relatively large phage pressure $P(0) > 10^8$ cm^{-3} is present. The broad minimum can span the time interval between 1 and 6 h after the phage is introduced. This behavior cannot be accurately accounted for by the dynamic equations without the switching terms as indicated by the simulated curves in Fig. 4, *b* and *e*. Here, we found that $S(t)$ recovers rather rapidly after the initial killing. Moreover, although the broad minimum seen in Fig. 3 was mimicked by the saddle-point approximation, to produce a good fit, the width of the receptor distribution σ was found to be twice as large as observed in the flow cytometry measurement. The broadened distribution exaggerates the size of the minority subpopulation; that is, to account for the very slow dynamics, it requires more minority cells with smaller n than are actually present in the bacterial population. We believe these discrepancies between theory and experiment are all stemmed from the inappropriate treatment of switching in the calculation. Indeed, as shown in Part I, in the presence of a very high $P(0) > 10^{10}$ cm^{-3} when all cells with finite n were expected to be decimated, we observed that the killing curves become independent of $P(0)$. In this extreme case, the killing curve can be interpreted as a slow leakage of cells from $n = 0$ to $n \neq 0$ states, and such a leakage appears to depend on whether the maltose operon is induced or not.

It should be kept in mind that since $S(t)$ is a sum over the bacterial subpopulations, it cannot provide direct information about how individual subpopulations react to $P(0)$ and how they switch. A quantity that is more closely related to the switching dynamics is the average adsorption rate $\bar{\gamma}_S(t) \equiv \sum_{n=0}^{N_{max}} \gamma_n S_n / S$ of sensitive cells, which may give us a closer look at the switching dynamics because $\bar{n}(t) \approx \bar{\gamma}_S(t)/\gamma_1$ reflects dynamics in the receptor space. According to Eq. 9, the time-dependent $S(t)$ and $P(t)$ allow us to calculate $\bar{\gamma}_S(t)$ a function of time:

$$\bar{\gamma}_S(t) = \frac{\Lambda - \Delta \ln S(t)/\Delta t}{P(t)}. \tag{18}$$

It should be emphasized that Eq. 9 was derived under the most general situation and consequently $\bar{\gamma}_S(t)$ derived using Eq. 18 is free of both the constant-P and no switching ($\alpha_{mn} = 0$) assumptions. Using the killing curve in Fig. 4 *a*, where both $S(t)$ and $P(t)$ were measured frequently in short time intervals, we were able to calculate $\Delta \ln S(t)/\Delta t$ using a cubic spline-interpolation method (20). The knowledge of $P(t)$ then allowed us to estimate the average adsorption rate constant $\bar{\gamma}_S$ as a function of time. Fig. 5 is a plot of $\bar{n}$ vs. t for three different initial phage concentrations $P(0) = 1 \times 10^9$ (*triangles*), 1×10^8 (*squares*), and 4×10^7 cm^{-3} (*circles*). Although the measurements are noisy, certain trends exist when $P(0)$ is varied. One observes that initially $\bar{n}(t)$ decreases with time, and the rate of decrease is enhanced as $P(0)$ increases. Moreover, the level of $\bar{n}(t)$ after several generations ($t > 2$ h) appears to depend on $P(0)$; it is $\bar{n} \sim 50$ for $P(0) = 4 \times 10^7$ cm^{-3} and $\sim$10 for $P(0) \sim 10^9$ cm^{-3}. We found in this intermediate-time regime, the condition $\Lambda_{eff} (\equiv \Lambda - \gamma_1 \bar{n} P) = 0$ is approximately satisfied, indicating that both $n(t)$ and $S(t)$ can reach a quasi-steady state simultaneously.

The fact that $\bar{\gamma}_S(t)$ or $\bar{n}$ or does not plummet to zero under a high phage pressure (MOI $\gg$ 1) is revealing, and it implies phenotype switching between subpopulations. By the definition of $\bar{\gamma}_S(t)$, it can be shown that the rate of change of $\bar{\gamma}_S(t)$ is given by

$$\dot{\bar{\gamma}}_S(t) \equiv \frac{\sum \gamma_i \dot{S}_i(t) - \bar{\gamma}_S(t)\dot{S}(t)}{S(t)}. \tag{19}$$

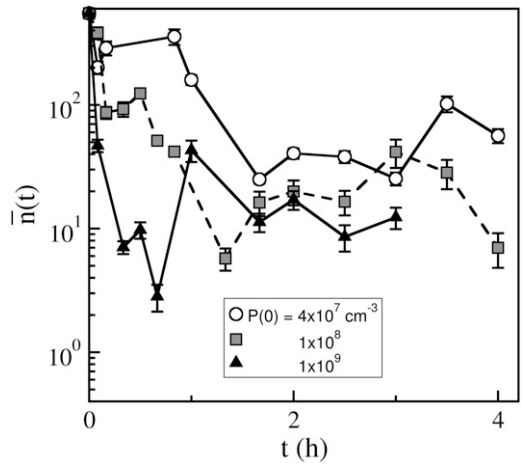

FIGURE 5 Time-dependent adsorption rate constant of the sensitive bacterial population. The $\bar{n}$ decreases with t when the phage pressure is applied. Here $\bar{n}$ was calculated using Eq. 1 based on measurements of $S(t)$ and $P(t)$. The three curves correspond to $P(0) = 1 \times 10^9$ (*triangles*), 1×10^8 (*squares*), and 4×10^7 cm^{-3} (*circles*). The bacterial concentration $B(0) = 3 \times 10^7$ cm^{-3} was the same for all runs.

The first term in the above equation can be calculated using Eq. 5 with the result

$$\frac{\sum \gamma_n \dot{S}_n(t)}{S(t)} = \Lambda \bar{\gamma}_S(t) - P(t)\overline{\gamma_S^2}(t) + \bar{D}(t), \qquad (20)$$

where $D_n = \sum_m (\gamma_m - \gamma_n)\alpha_{mn}$ and the over-bar is the average according to the distribution $p(n,t) = S_n(t)/S(t)$. Physically, $\bar{D}(t)$ represents the mean spreading rate in the receptor space. It is evident that in the absence of a phage pressure $\bar{D}(t) = 0$ because $p(n,t)$ is time-invariant. On the other hand, when $P(0) \neq 0$, preferential killing causes $\bar{D}(t)$ to be more heavily weighed for small n than for large n, giving rise to $\bar{D} > 0$. Since $\dot{S}(t)/S(t) = \Lambda - \bar{\gamma}_S(t)P(t)$, substituting Eq. 20 into Eq. 19, we finally arrive at the relation

$$\dot{\bar{\gamma}}_S(t) = -\sigma_\gamma^2(t)P(t) + \bar{D}(t), \qquad (21)$$

where $\sigma_\gamma^2(t) \equiv \overline{\gamma_S^2}(t) - \bar{\gamma}_S(t)^2$ is the variance of the adsorption constant. We note that if there is no phenotype switching $\bar{D} = 0$, $\bar{\gamma}_S(t)$ can only decrease with time for σ_γ^2 being positive. Asymptotically, therefore, $\bar{\gamma}_S$ should approach zero or correspondingly $\bar{n} \to 0$. A small but finite $\bar{n}$ observed in the experiment even after persistent phage pressure $P(t) \sim 1 \times 10^8$ cm^{-3} demands that the switching rates between bacterial subpopulations must not be zero at least within our observation time of ~4 h. It should be emphasized that Eq. 21 is the dynamic equation for the receptors, and its relation to the sensitive bacterial population is a delicate one. This has to be the case because the interaction between a phage and its receptor is essentially a ''chemical'' process determined by the law of mass action, whereas the life-and-death of a bacterium is a highly nonlinear biological process. It remains an intriguing possibility that in a long time, the receptor number may reach a ''chemical equilibrium'' with $\dot{\bar{\gamma}}_S(t) \approx 0$ (or $\dot{\bar{n}} = 0$), yielding $\bar{D}(t) \approx \sigma_\gamma^2 P(t)$. However, the average receptor number $\bar{n}$ in such a state is so small that the growth rate $\Lambda_{eff} (\equiv \Lambda - \gamma_1 \bar{n} P)$ for the sensitive cells is positive, giving rise to exponential growth of $S(t)$. Whether this is what happened in our late-time bacterium/phage population dynamics remains to be verified by future experiments.

For a simple application of Eq. 21, we noted that it allows us to explain the killing data beyond the initial exponential behavior, i.e., within the first few minutes of measurements. This is because for early times $\sigma_\gamma^2(0)$ is expected to be a constant and $\bar{D}(0) = 0$, since the receptor distribution is still at the steady state. A simple integration yields $\bar{\gamma}_S(t) = \bar{\gamma}_S(0) - \sigma_\gamma^2(0)P(0)t$. Substituting this relation into Eq. 9 and integrating over t again, we found

$$S(t) \approx S(0)\exp\left[(\Lambda - \bar{\gamma}_S(0)P(0))t + \frac{1}{2}\sigma_\gamma^2(0)P(0)^2 t^2\right]. \qquad (22)$$

In the short-time limit, this equation turns out to be the same as Eq. 16, which was derived without the switching terms. The new derivation in Eq. 22 lends support to our earlier assertion that phenotype switching is important only for the intermediate- to the long-time behavior of the bacterial population. By varying $P(0)$ systematically, Eq. 22 can be used to find $\bar{\gamma}_S(0)$ and its standard deviation $\sigma_\gamma(0)$. Equation 22 also suggests the following scaling relation: $\Phi(s) = (1/t \ln S(t)/S(0) - \Lambda_{eff})/C = t$, where $\Lambda_{eff} = \Lambda - \gamma_S(0)P(0)$ and $C = \frac{1}{2}\sigma_\gamma(0)^2 P(0)^2$. One thus expects that if the early-time killing curves $S(t)$ are normalized and parameters Λ_{eff} and C are properly chosen, all the killing data should be collapsed onto a single/universal line with a slope of unity. We demonstrated this scaling procedure using the data from both strains of bacteria when $P(0)$ was varied between 1.2×10^8 to 5.3×10^8 cm^{-3} for LE392, and when $P(0)$ was varied between 1.2×10^8 to 1.0×10^9 cm^{-3} for Ymel. The symbols in Fig. 6 *a* are the original data of LE392, and the scaled curves are displayed in Fig. 6 *b* as open symbols, along with the measurements of Ymel bacteria (*solid symbols*). We found that our data collapse well only for times $<\sim 300$ s, which is consistent with the theoretical prediction since for $t \gg \Lambda_{eff}/C$, Eq. 22 is no longer valid. The above scaling procedure also allows us to verify the linear and quadratic relationships between Λ_{eff} and C with $P(0)$, which are plotted in Fig. 6, *c* and *d*. Based on this analysis, we found that the average adsorption coefficient and its variance are given by $\bar{\gamma}_S = (1.7 \pm 0.2) \times 10^{-11}$ cm^3/s and $\sigma_\gamma = (1.12 \pm 0.07) \times 10^{-11}$cm^3/s for Ymel, and $\bar{\gamma}_S = (4.6 \pm 0.5) \times 10^{-11}$ cm^3/s and $\sigma_\gamma = (2.2 \pm 0.2) \times 10^{-11}$ cm^3/s for LE392. Using Berg and Purcell's prediction in Eq. 1, $\bar{\gamma}_S(0)$ and $\sigma_\gamma^2(0)$ can be converted to $\bar{n}$ and σ_n. We found that $\bar{n}$ and σ_n extracted in this fashion are in reasonably good agreement with the flow cytometry measurements as delineated in Table 1.

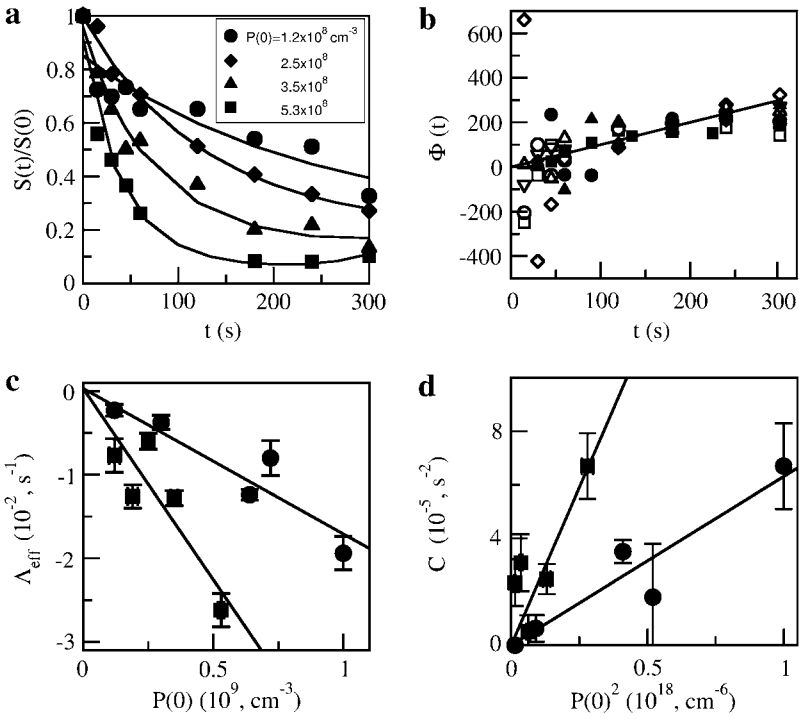

FIGURE 6 Short-time (<5 min) killing curves for Ymel and LE392. (*a*) Examples of short-time killing curves for LE392 with initial phage concentrations of $P(0) = 1.2 \times 10^8$ cm^{-3} (*circles*); 2.5×10^8 cm^{-3} (*diamonds*); 3.5×10^8 cm^{-3} (*triangles*) ; and 5.3×10^8 cm^{-3} (*squares*). Lines are guides to the eye. (*b*) Nine different killing curves, such as the ones displayed in panel *a*, can be collapsed onto a straight line characterized by the equation $\Phi(s) = \left[\frac{1}{t}\ln(S(t)/S(0)) - \Lambda_{\text{eff}}\right]/C = t$. Here data from both LE392 (*open symbols*) and Ymel (*solid symbols*) bacteria were used. (*c* and *d*) The circles and the squares are, respectively, for Ymel and induced LE392 bacteria. The parameters Λ_{eff} and C are defined in the equation for $\Phi(s)$, shown in this legend. The slopes in panels *c* and *d* allow $\bar{\gamma}(0)$ and $\sigma_\gamma(0)$ to be calculated (see main text), and their values are listed in Table 1.

CONCLUSION

We have presented a theoretical model taking into account known interactions between bacterium and phage. A distinguishable feature of our model is the division of bacteria into subpopulations depending on their phage receptor numbers. For a narrow receptor distribution, this heterogeneous model can be reduced to the standard homogeneous one that is typically used in the literature. It is also shown that while the homogeneous model lacks the plasticity for the bacterial population to coexist with a phage population, which typically leads $S(t)$ to extinction in long times, the heterogeneous model is much more robust and $S(t)$ does not become extinct unless a persistent, high phage pressure is present. This is consistent with our experimental observation in Part I where mutants are present in significant numbers only when a large pressure of $P(0) > 10^{10}$ cm^{-3} is applied.

The Berg-Purcell's theoretical result for the phage adsorption rate allows the cell states to be enumerated, and the statistical properties of birth/death rates to be calculated for the heterogeneous bacterial population. It is surprising that statistical fluctuations in the receptor number alone appears to account for the main features of bacterium/phage population dynamics, including the coexistence of the two species over a broad range of phage pressures. The improved fitness in the heterogeneous population results from the fact that in the presence of phage, the high-n cells are preferentially infected. In the case when the MOI is much less than the average number of receptors per bacterium $\bar{n}$, the high-n cells also effectively shield low-n cells from phage attack, allowing the latter to grow despite the phage pressure. At the population level, the improved fitness is manifested by a time-dependent adsorption rate $\bar{\gamma}_S(t)$ that decreases with time until the effective growth rate $\Lambda_{\text{eff}} = \Lambda - \bar{\gamma}_S(t)P(t)$ becomes positive at a long time. Interestingly, our experiment shows that the transition from $\Lambda_{\text{eff}} < 0$ to $\Lambda_{\text{eff}} > 0$ takes a very long time (4–5 h), and in the intervening period, the system appears to be locked in a quasi-steady state with $\Lambda_{\text{eff}} = 0$. This behavior cannot be accounted for by the receptor-number heterogeneity alone, and it appears that phenotype switching is essential for the observed quasi-steady state. In our opinion, the time-dependent $\bar{\gamma}_S(t)$ in the presence of a phage pressure is an important observation of this experiment. It invalidates an important assumption in early bacterium/phage population models: which assume $\bar{\gamma}_S(t)$ to be a constant having the same value $\bar{\gamma}_S(0)$ determined from a unstressed population. The experiment herein demonstrates that $\bar{\gamma}_S(t)$ can change by orders of magnitude under a phage stress.

While the full model presented by Eqs. 5–7 is complex, it admits solutions when certain approximations are made, such as when 1), the phage pressure is so high that it can be considered as constant; 2), no phenotype switching is present; and 3), the short- and perhaps the intermediate-time limits are considered. We found that for slow switching rates, the approximations 2 and 3 are equivalent, yielding similar solutions for $S(t)$ as delineated by Eqs. 14 and 22. These approximations are admittedly rather crude, but they can reproduce qualitative behaviors that are consistent with the observations, suggesting that population heterogeneity is an essential feature of bacterium/phage population dynamics. In the short-time limit, however, these equations can yield

quantitative results as demonstrated by their predictive power for $\bar{n}$ and σ_n as delineated in Fig. 6. Perhaps the most significant result of the theoretical analyses is the prediction: $\dot{\bar{\gamma}}_S(t) = -\sigma_\gamma^2(t)P(t)+\bar{D}(t)$. The first term in this equation causes the average adsorption rate to decrease with time while the second term causes it to increase. Since our measured $\bar{\gamma}_S(t)$ never approaches zero after several hours of phage stress for a variety of $P(0)$, it provides evidence that phenotype switching must take place or $\bar{D}$ must not be zero for our bacterium/phage system.

Since the comparison between theory and experiment is only qualitative at the present level of analysis, particularly for the intermediate- and long-times, there is ample room for future improvements. It appears that the most important missing piece is the biological mechanism for phenotype switching. This requires both experimental and theoretical efforts to sort out. Experimentally, a better understanding of LamB protein dynamics, i.e., the synthesis, folding, receptor assembly, and partitioning during cell division, is urgently needed. Theoretically, the presentation of the population dynamic equations by a set of ordinary differential equations is highly inconvenient. It would be useful to develop a coarse-grained model in the spirit of balanced-population models, which have been successfully used for describing stochastic bacterial cell division (23). However, how to rationally couple the random protein dynamics of interest, such as our LamB, with the cell growth/division parameter remains to be investigated. New insights may also be gained by investigating the regulation of the maltose regulon, which appears to operate differently from the more commonly studied lactose or arabinose regulatory systems (24,25). It has been recognized by early genetic studies that MalT, which is a positive regulator of the maltose regulon, is not self-regulated and its expression is limited both at the transcription and translation levels (26,27). This regulation scheme is peculiar because it suggests that the regulon is intrinsically noisy. While it makes sense in most circumstances for a gene circuit to minimize stochastic fluctuations, noisy gene regulation can in other circumstances be advantageous particularly when organisms are subject to fluctuating environmental stresses (28). In the present case of maltose regulon, the stochasticity would allow the cell population to prosper in very low concentrations of maltose while still able to face the challenge of λ-phage. Thus, it remains an intriguing possibility that evolution of maltose regulon is strongly influenced by the selection pressures of bacterial viruses, such as λ, K10, and TPI, which exploit the maltose receptor LamB (29). Theoretically, it will be very useful to model the maltose regulon to see if the broad LamB distribution can result from its peculiar regulation mechanism.

SUPPLEMENTARY MATERIAL

To view all of the supplemental files associated with this article, visit www.biophysj.org.

We appreciate many useful discussions with Chuck Yeung to clarify a number of ideas in the model.

This work was supported by the National Science Foundation under grant No. PHY-0646573. E.C-M.. acknowledges partial support by the National Science Foundation during this project as a GK-12 Fellow under grant No. 0338135 (GK-12: The Pittsburgh Partnership for Energizing Science in Urban Schools).

REFERENCES

1. Elowitz, M. B., A. J. Levine, E. D. Siggia, and P. S. Swain. 2002. Stochastic gene expression in a single cell. *Science*. 297:1183–1186.
2. Raser, J. M., and E. O'Shea. 2005. Noise in gene expression: origins, consequences and control. *Science*. 309:2010–2013.
3. Halme, A., S. Bumgarner, C. Styles, and G. R. Fink. 2004. Genetic and epigenetic regulation of the FLO gene family generates cell-surface variation in yeast. *Cell*. 116:405–415.
4. Pedraza, J. M., and A. van Oudenaarden. 2005. Noise propagation in gene networks. *Science*. 307:1965–1969.
5. Balaban, N. Q., J. Merrin, R. Chait, L. Kowalik, and S. Leibler. 2004. Bacterial persistence as a phenotypic switch. *Science*. 305:1622–1625.
6. Kussell, E., R. Kishnoy, N. Q. Balaban, and S. Leibler. 2005. Bacterial persistence: a model of survival in changing environment. *Genetics*. 169:1807–1814.
7. Thattai, M., and A. van Oudenaarden. 2004. Stochastic gene expression in fluctuating environments. *Genetics*. 167:523–530.
8. Cai, L., N. Friedman, and X. S. Xie. 2006. Stochastic protein expression in individual cells at the single molecule level. *Nature*. 440:358–362.
9. Ryter, A., H. Shuman, and M. Schwartz. 1975. Integration of the receptor for bacteriophage-λ in the outer membrane of *Escherichia coli*: coupling with cell division. *J. Bacteriol*. 122:295–301.
10. Levin, B. R., F. M. Stewart, and L. Chao. 1977. Resource-limited growth, competition and predation: a model and experimental studies with bacteria and bacteriophage. *Am. Nat*. 111:3–24.
11. Chao, L., B. R. Levin, and F. M. Steward. 1977. A complex community in a simple habitat: an experimental study with bacteria and phage. *Ecology*. 58:369–378.
12. Lenski, R. E., and B. R. Levin. 1985. Constraints on the coevolution of bacteria and virulent phage: a model, some experiments, and predictions for natural communities. *Am. Nat*. 125:585–602.
13. Moldovan, R., E. Chapman-McQuiston, and X. L. Wu. 2007. On kinetics of phage adsorption. *Biophys. J*. 93:303–315.
14. Rabinovitch, A. 2003. Bacterial debris—an ecological mechanism for coexistence of bacteria and their viruses. *J. Theor. Biol*. 224:377–383.
15. Berg, H. C., and E. M. Purcell. 1977. Physics of chemoreception. *Biophys. J*. 20:193–219.
16. Schwartz, M. 1976. The adsorption of coliphage-λ to its host: effect of variation in the surface density of receptor and in phage-receptor affinity. *J. Mol. Biol*. 103:521–536.
17. Zwanzig, R. 1990. Diffusion-controlled ligand binding to spheres partially covered by receptors: an effective medium treatment. *Proc. Natl. Acad. Sci. USA*. 87:5856–5857.
18. Wangersky, P. J. 1978. Lotka-Volterra population models. *Annu. Rev. Ecol. Syst*. 9:189–218.
19. Szmelcman, S., and M. Hofnung. 1975. Maltose transport in *Escherichia coli* K-12: involvement of the bacteriophage λ-receptor. *J. Bacteriol*. 124:112–118.
20. Press, W. H., S. A. Teukolsky, W. T. Vetterling, and B. P. Flannery. 1988. Numerical Recipes in C: The Art of Scientific Computing. Cambridge University Press, New York.
21. Banerjee, B., S. Balasubramanian, G. Ananthakrishna, T. V. Ramakrishnan, and G. V. Shivashankar. 2004. Tracking operator state fluctuations in gene expression in single cells. *Biophys. J*. 86:3052–3059.

22. Krishna, S., B. Banerjee, T. V. Ramakrishnan, and G. V. Shivashankar. 2005. Stochastic simulations of the origins and implications of long-tailed distributions in gene expression. *Proc. Natl. Acad. Sci. USA*. 102:4771–4776.

23. Ramkrishna, D. 2000. Population Balances: Theory and Applications to Particulate Systems in Engineering. Academic Press, San Diego, CA.

24. Novick, A., and M. Weiner. 1957. Enzyme induction as an all-or-none phenomenon. *Proc. Natl. Acad. Sci. USA*. 43:553–566.

25. Siegele, D., and J. C. Hu. 1997. Gene expression from plasmids containing the araBAD promoter at subsaturating inducer concentration represents mixed populations. *Proc. Natl. Acad. Sci. USA*. 94:8168–8172.

26. Chapon, C. 1982. Expression of MalT, the regulator gene of the maltose regulon in *Escherichia coli*, is limited both at transcription and translation. *EMBO J*. 1:369–374.

27. Schwartz, M. 1987. The maltose regulon. *In Escherichia coli* and *Salmonella typhimurium*, Cellular and Molecular Biology. F. C. Neidhardt, Editor. American Society for Microbiology, Washington, DC.

28. Bar-Even, A., J. Paulsson, N. Maheshri, M. Carmi, E. O'Shea, Y. Pilpel, and N. Barkai. 2006. Noise in protein expression scales with natural protein abundance. *Nat. Genet*. 38:636–643.

29. Schwartz, M. 1980. Interaction of phages with their receptor proteins. *In* Virus Receptors. Receptors and Recognition, B Series. L. L. Randall and L. Philipson, Editors. Chapman and Hall, London.